Chemical Science

Accepted Manuscript

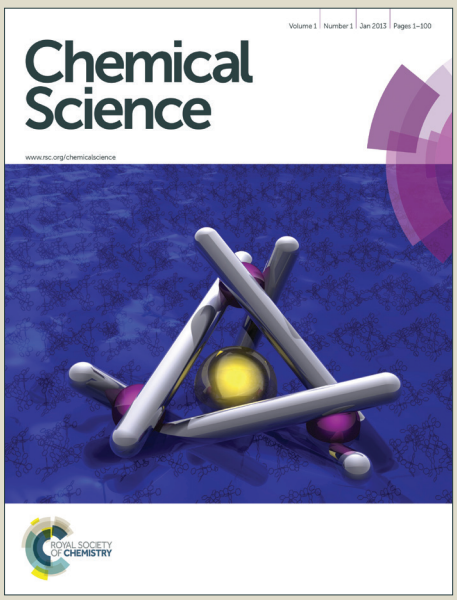

ROYAL SOCIETY OF CHEMISTRY

www.rsc.org/chemicalscience

Cite this: DOI: 10.1039/c0xx00000x

www.rsc.org/xxxxxx

ARTICLE TYPE

Bioinspired polydopamine nanospheres: a superquencher for fluorescence sensing of biomolecules

Weibing Qiang, Wei Li, Xiaoqing Li, Xiang Chen, Danke Xu*

Received (in XXX, XXX) Xth XXXXXXXXX 20XX, Accepted Xth XXXXXXXXX 20XX

DOI: 10.1039/b000000x

The high fluorescence quenching ability for a wide spectrum of fluorescent dyes of bioinspired polydopamine nanospheres was shown for the first time. Up to 97% quenching efficiency via energy transfer and/or electron transfer was obtained toward four kinds of fluorophores, Aminomethylcoumarin Acetate (AMCA), 6-Carboxyfluorescein (FAM), 6-Carboxytetramethylrhodamine (TAMRA) and Cy5. This fluorescence quenching ability was compared favorably with graphene oxide, the superquencher. And the nanospheres (NS) exhibit different affinities to various ssDNA conformations. Furthermore, FAM-labeled ssDNA was adsorbed onto NS through non-covalently binding to form an ssDNA/NS complex, leading to the quenching of the fluorescence of FAM. This complex was used as a sensing platform for detection of DNA and proteins based on the fluorescence recovery due to the targets recognition. The LOD of DNA and thrombin were equal or close to GO-based biosensors. The assay is fast, simple and homogeneous, which could be used for fluorescence imaging. And the excellent biocompatibility and biodegradability of polydopamine make it suitable for *in vivo* applications.

Introduction

Rapid, cost-effective, sensitive and specific analysis of biomolecules is important in the fields of drug discovery, environmental monitoring, food safety, clinical diagnostics and treatment. The development of fluorescent sensors for assaying biomolecules has recently received considerable attention due to their inherent advantages, such as high sensitivity, operational convenience, and especially the *in situ* imaging property.[1, 2] This type of sensors usually consist of a fluorophore and a quencher to form a Förster resonance energy transfer (FRET) pair, in which the distance-dependent fluorescence quenching is closely coupled with the biomolecular recognition event. Based on this signal-transduction mechanism, as one kind of hairpin-structured DNA probes, molecular beacons are elaborately designed.[3-5]

Owing to their unique optical, electronic, and catalytic properties, nanomaterials have been used as novel biosensing platforms.[6-8] Over the past few years, many nanomaterial-based fluorescent biosensors have been exploited by using nanomaterials as quenchers. These nanoquenchers are available to eliminate the selection issue of a fluorophore–quencher pair, due to their ability to quench fluorophores with different emission frequencies, and improve the signal-to-noise ratio of DNA probes. Gold nanoparticles (AuNPs),[9, 10] carbon nanomaterials including 0D carbon nanoparticles (CNPs),[11, 12] 1D carbon nanotubes (CNTs),[13, 14] and 2D graphene oxide (GO),[15, 16] and recently developed metal-organic framework (MOF)[17] and MoS_2 nanosheets[18] have been used as highly efficient nanoquenchers to develop novel fluorescent sensors. Although these nanoquenchers have been successfully used for the detection of nucleic acids, proteins, metal ions, small molecules and enzymes,[19-27] the preparations of some materials are often elaborate and fussy, and some of the materials are toxic for *in vivo* studies; therefore, the current researches have been focused on developing new materials as replacements.

Bioinspired polydopamine (PDA) is a dopamine derived synthetic eumelanin polymer with excellent biocompatiblity and biodegradability, which is widely distributed throughout the human body. PDA is the first polymer reported that can independently functionalize surfaces made of virtually all materials.[28] Due to this fantastic feature, it has been extensively investigated for various applications including surface modification, metal deposition, drug delivery and others.[29-39] Most of the studies are focused on the coating property, the fluorescence quenching ability of PDA have not been reported yet.

In this work, the fluorescence quenching ability of polydopamine nanospheres (PDANSs) was studied. It was found that the quenching ability was equivalent to graphene oxide and the quenching action was through energy transfer and/or electron transfer. Due to the interaction between ssDNA and PDANSs, 6-Carboxyfluorescein (FAM) labeled ssDNA was adsorbed onto PDANSs to form a complex, leading to the quenching of fluorescence. And this complex was adopted as a sensing platform to detect DNA and proteins based on the fluorescence recovery lead by the targets recognition. As the sensing of the biomolecules is fast and simple, this sensing platform could be used for the assay of other targets. And this will also broaden the application of polydopamine in the life science.

Results and discussion

In our experiments, polydopamine nanospheres were synthesized in a mixed solvent of Tris-buffer and isopropyl alcohol, according to a reported method with modifications.[40] In an alkaline environment, the oxidation of catechol is considered to lead the self-polymerization of dopamine (Fig. 1A). We prepared the monodisperse polydopamine nanospheres NS-1 with a diameter of approximately 336.0 nm through a facile and low-cost method (Fig. 1B). Complementary to IR and Raman spectra, which were consistent with those in another report,[41] provided evidence of successful PDANSs synthesis (Fig. 1C,D). The obtained NS-1 had a zeta potential of -55.5 mV and were well-dispersed in water.

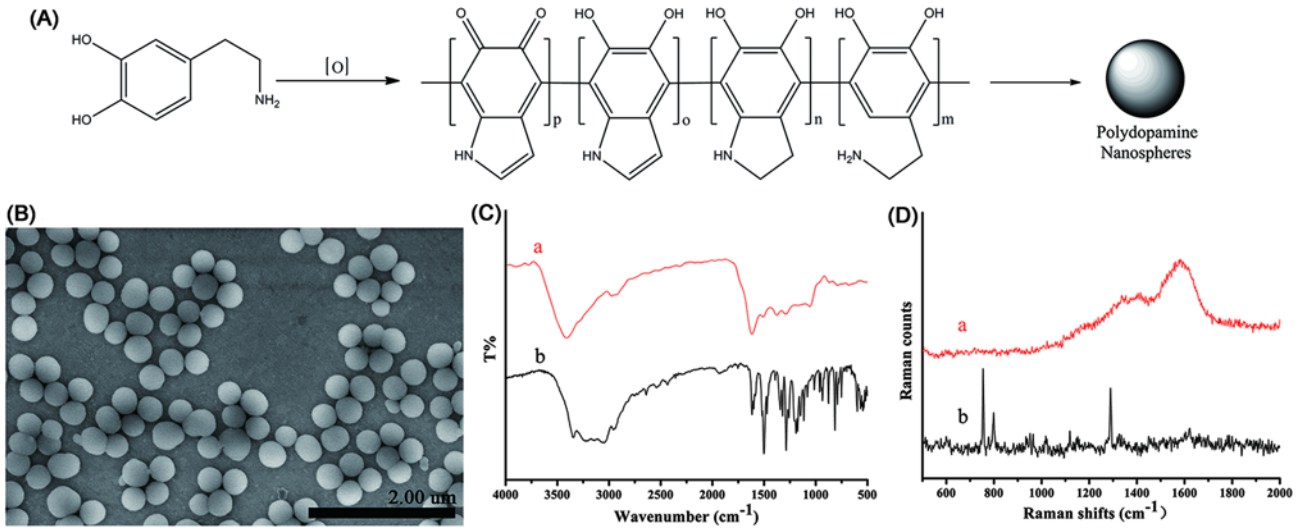

Fig. 1 (A) Simplified schematic of the oxidative polymerization of dopamine to prepare polydopamine nanospheres. (B) SEM image of NS-1, the diameter is 336.0±37.5 nm. (C) IR spectra of (a) NS-1 and (b) dopamine. (D) Raman spectra of (a) NS-1 and (b) dopamine.

Table 1 Detailed DNA sequence information[a]

Name	Sequence (5' to 3')
P-AMCA	AMCA-GGTTGGTGTGGTTGG
P-FAM	FAM-GGTTGGTGTGGTTGG
P-TAMRA	TAMRA-GGTTGGTGTGGTTGG
P-Cy5	Cy5-GGTTGGTGTGGTTGG
T1	CCAACCACACCAACC
T2	CCATCCAGACCTACC
M1	CCAACCAGACCAACC
M2	CCAACCAAACCAACC
M3	CCAACCATACCAACC
P-A	FAM-AAAAAAAAAAAAAAA
P-T	FAM-TTTTTTTTTTTTTTT
P-C	FAM-CCCCCCCCCCCCCCC
P-3FAM	GGTTGGTGTGGTTGG-FAM
T-A	AAAAAAAAAAAAAAA
T-T	TTTTTTTTTTTTTTT

[a] The mismatched bases in comparison with T1 are underlined.

The fluorescence quenching ability of the monodisperse polydopamine nanospheres NS-1 was shown in Fig. 2B-E and S2. In the absence of NS-1, four types of probe DNAs with different fluorophores, Aminomethylcoumarin Acetate (AMCA), 6-Carboxyfluorescein (FAM), 6-Carboxytetramethylrhodamine (TAMRA) and Cy5, labeled at 5' end have strong fluorescence emission. The introduction of NS-1 would bind with probe DNAs and quenched the fluorescence of the fluorophores. And the quenching efficiency (QE) was more than 97% toward all those four fluorophores. Moreover, the fluorescence of FAM on the probe DNAs with different sequences was also quenched efficiently (> 94%) (Fig. S2A-C). As shown in Fig. S2D, the fluorescence of FAM labeled on 3' terminal of P-3FAM was quenched, and this indicated that the quenching ability of PDANSs was independent with the location of the fluorophores.

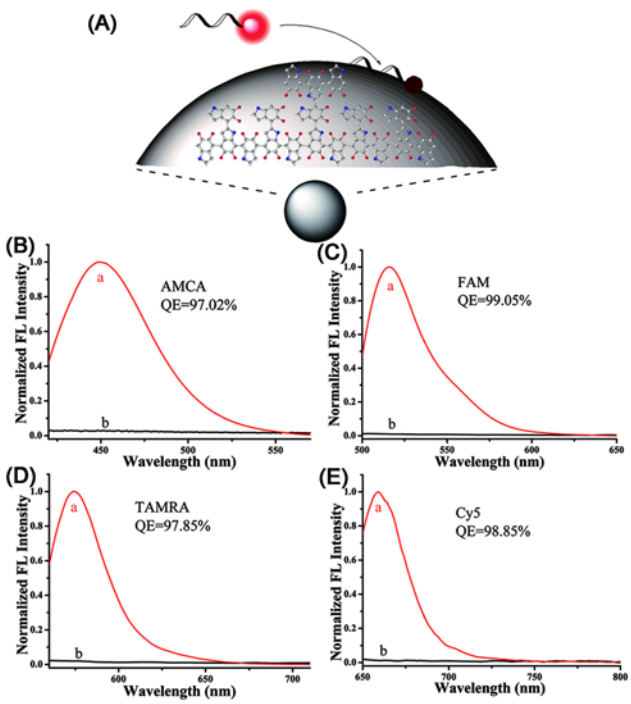

Fig. 2 (A) The scheme of the fluorescence quenching of probe DNA by PDANSs. (B) Fluorescence emission spectra of probe DNA (a) P-AMCA and (b) P-AMCA in the presence of NS-1. (C) Fluorescence emission spectra of probe DNA (a) P-FAM and (b) P-FAM in the presence of NS-1. (D) Fluorescence emission spectra of probe DNA (a) P-TAMRA and (b) P-TAMRA in the presence of NS-1. (E) Fluorescence emission spectra of probe DNA (a) P-Cy5 and (b) P-Cy5 in the presence of NS-1.

Those demonstrated that PDANSs illustrated high fluorescence

quenching efficiency. And the quenching action was fast, toward P-FAM, with up to 99% quenching efficiency was obtained within 60 s after the introduction of NS-1 (Fig. S3).

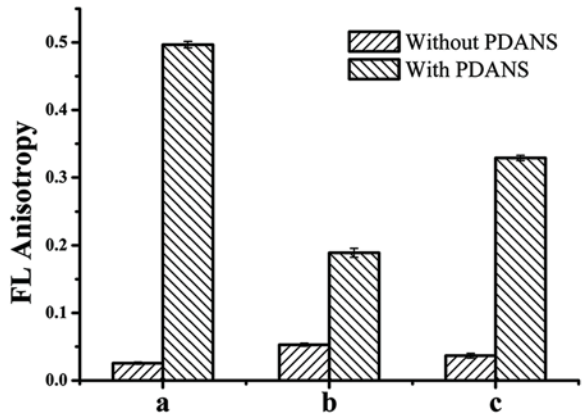

Fig. 3 Fluorescence anisotropy of (a) P-FAM, (b) P-FAM/T1, (c) P-FAM/Thrombin, and in the presence of NS-1.

Anisotropy measurements are commonly used to investigate molecular interactions. As shown in Fig. 3, the fluorescence anisotropy of free P-FAM in buffer was 0.026, and it increased 19.12-fold after introduction of NS-1, indicating that P-FAM was adsorbed on the surface of PDANSs. Though the detail of the structure of PDA is still under discussion, it was deemed that PDA is composed of dihydroxyindole, indoledione, and dopamine units.[42-44] The units condense to oligomers through covalently bonding, and these oligomers then aggregate through π-π stacking to form 1-2 nm sized plate-like aggregates, which further π-stack to second and third level aggregates of tens to hundreds of nanometers in diameter.[45] The interaction between PDANSs and ssDNA was possibly led by the non-covalently binding through multi-contact points of long strands due to hydrogen bonding, π-π stacking, or charge-transfer complexes between the units of PDA and nucleobases. However, the detailed interaction mechanism is still not fully understood.[29, 30]

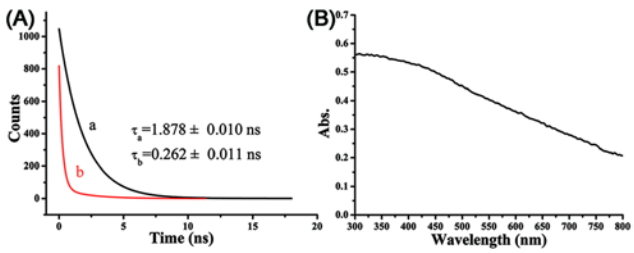

Fig. 4 (A) Fluorescence decay curves of (a) P-Cy5 and (b) P-Cy5 in the presence of NS-1. (B) Uv-visible spectrum of NS-1.

For the quenching mechanism, the change of Cy5's fluorescence decay time from 1.878 ns to 0.262 ns, before and after introduction of NS-1, indicated the quenching of fluorescence possibly through a dynamic theory (Fig. 4A). While the Stern-Volmer plot showed a nonlinear correlation and is an upward curvature, concave toward the y-axis (Fig. S4). These demonstrated that the quenching was the combination of dynamic and static quenching. As NS-1 show broad band absorbance in UV-Vis spectrum that lead to a spectral overlap with the emission spectra of fluorophores (Fig. 4B), PDANSs would quench the fluorescence of those fluorophores due to the FRET. On the other hand, the monomer dopamine and its oxide quinone, proved existing in PDA,[42] have shown the quenching ability toward fluorophores and QDs via photoinduced electron transfer (PET).[46-48] And the fluorescence of the probe DNA was quenched by dopamine with some level (Fig. S5), the role of electron transfer in the fluorescence quenching could not be ruled out. Hence, the quenching action was through energy transfer and/or electron transfer.

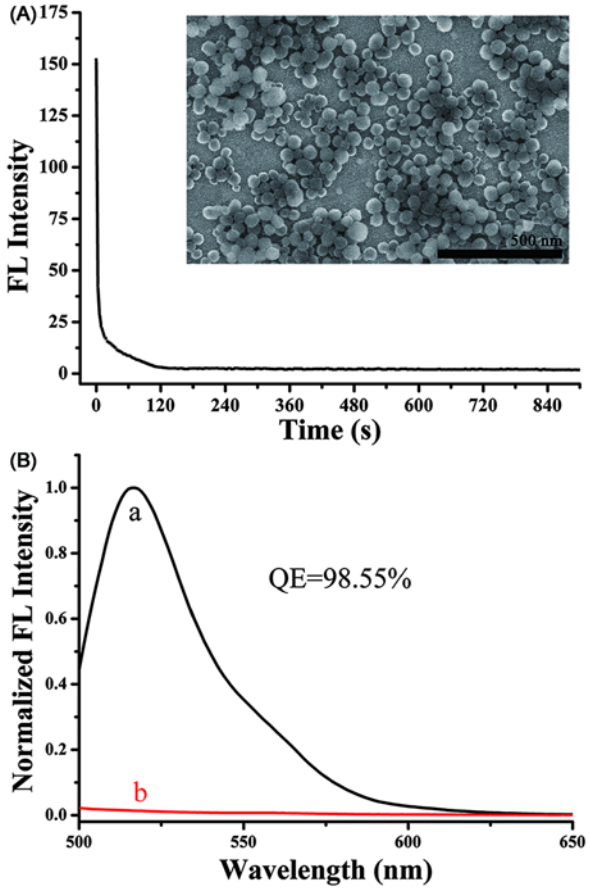

Fig. 5 (A) Fluorescence quenching of P-FAM in the buffer by NS-2 as a function of time. Inset: SEM image of NS-2, the diameter is 54.0±6.6 nm. (B) Fluorescence emission spectra of probe DNA (a) P-FAM and (b) P-FAM in the presence of NS-2.

As the size of PDANSs could be easily controlled by tuning the molar ratio of buffer to alcohol and the polymerization time, NS-2 with the diameter of about 54.0 nm, which was similar with the reported size of CNPs, was obtained by controlling those conditions (Fig. 5A). While, the quenching kinetics of NS-2 was faster; the time to reach equilibrium was approximately 2 minutes, comparing to over 15 minutes of CNPs. Additionally, the quenching efficiency of NS-2 was over 98%, which was higher than that of CNPs at approximately 90%.[49, 50] (Fig. 5) So that, the fluorescence quenching ability of PDANSs should be better than CNPs. As high quenching efficiency (> 98%) was also obtained for the other size of PDANSs (Fig. S7), PDANSs exhibited glaring fluorescence quenching ability, which was better than the commonly used AuNPs and compared favorably with the outstanding carbon nanomaterials.[51]

As shown in Fig. 3, the fluorescence anisotropy of P-FAM/T1 increased less than that of the P-FAM after the introduction of NS-1, suggesting the interaction between dsDNA and NS-1 was weaker. And this phenomenon also existed in P-FAM/Thrombin, as P-FAM is the aptamer against human thrombin, they presented as a complex due to the specific aptamer-target recognition. The different affinities of PDANSs toward various ssDNA conformations were caused by the change of the interactions between the nucleobases and PDANSs. When the conformation of ssDNA changed, the approaching of the nucleobases toward PDANSs was impeded, and then the interaction was weakened.

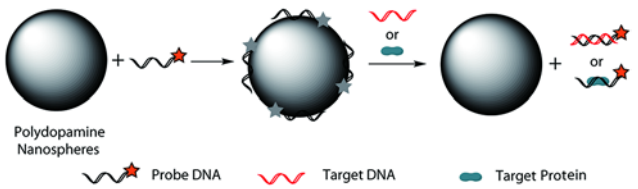

Scheme 1 The principle of the sensing of the biomolecules.

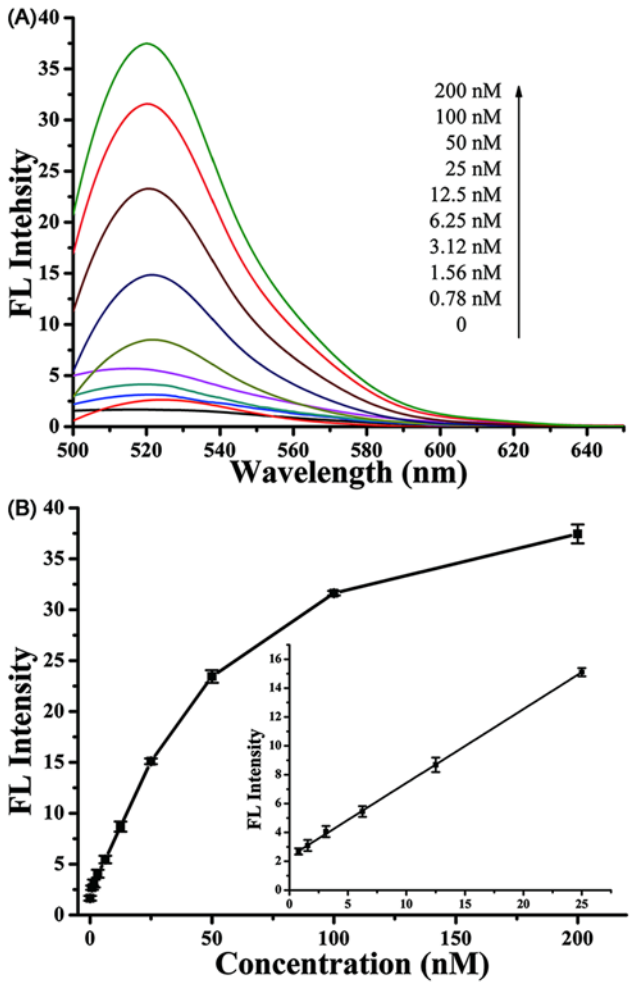

Fig. 6 (A) Fluorescence emission spectra of P-FAM/NS-1 in the presence of different concentration of T1 (0, 0.78, 1.56, 3.12, 6.25, 12.5, 25, 50, 100, and 200 nM). (B) Calibration curve for DNA detection. Inset: amplification of the low concentration range of the calibration curve.

For the high fluorescence quenching efficiency and variational affinities toward various ssDNA conformations, PDANSs could be used to construct a platform for the detection of a broad range of analytes. The principle of this sensing strategy is shown in Scheme 1. In the absence of NS-1, free probe DNA P-FAM had a strong fluorescence emission at 518 nm. The introduction of NS-1 would bind with probe DNA to form a P-FAM/NS-1 complex and quenched the fluorescence of FAM. While, after the introduction of targets, the complementary DNA T1 or thrombin, they reacted with P-FAM, and the conformation of P-FAM changed. P-FAM would be released from PDANSs due to the weakened interaction between them, resulting in the recovery of fluorescence of FAM. Hence, the restoration of fluorescence can be applied to quantitative analysis of DNA and thrombin.

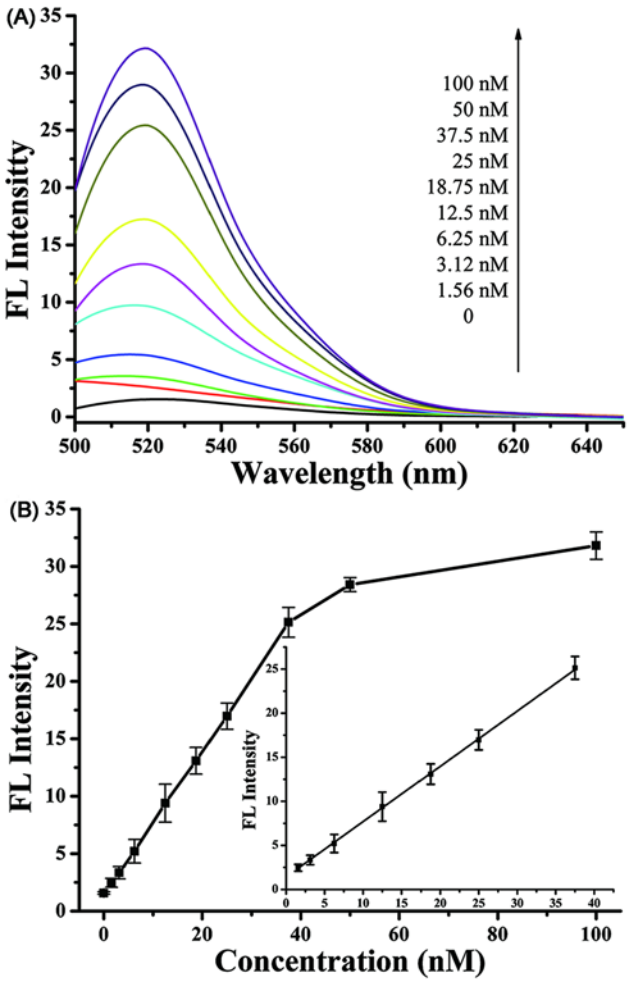

Fig. 7 (A) Fluorescence emission spectra of P-FAM/NS-1 in the presence of different concentration of thrombin (0, 1.56, 3.12, 6.25, 12.5, 18.75, 25, 37.5, 50, and 100 nM). (B) Calibration curve for thrombin detection. Inset: amplification of the low concentration range of the calibration curve.

As mentioned above, the assay of DNA was carried out. With the increased concentration of T1, more P-FAM was released from the surface of NS-1. As a result, the retained fluorescence of P-FAM was intensified (Fig. 6A). Hence, the fluorescence intensity can be used to monitor the concentration of DNA. This DNA sensor showed a linear relationship ranged from 0.78 to 25 nM, with a detection limit of 0.1 nM (Blank + 3 SD) (Fig. 6B). The detection limit of ssDNA was found to be equal to the reported GO-based sensors,[52, 53] but better than many other nanoquencher-based sensors.[11, 13, 17, 18] As the fluorescence of some other probe DNA/NS-1 was enhanced in the presence of the corresponding

target DNA, the universality of this DNA sensing platform was proved (Fig. S8).

Herein, PDANSs as a sensing platform was recruited for the detection of human thrombin. As expected, the fluorescence recovery was observed after the introduction of thrombin. Fig. 7A showed the fluorescence emission spectra of P-FAM/NS-1 in the presence of different concentrations of thrombin. The fluorescence intensity was found to be linear with the concentrations in the range of 0.78-37.5 nM (Fig. 7B). The limit of thrombin detection was estimated to be 0.5 nM (Blank + 3 SD), which was lower than most of the nanoquencher-based sensors[15, 17, 54] and close to the GO-based sensor[55].

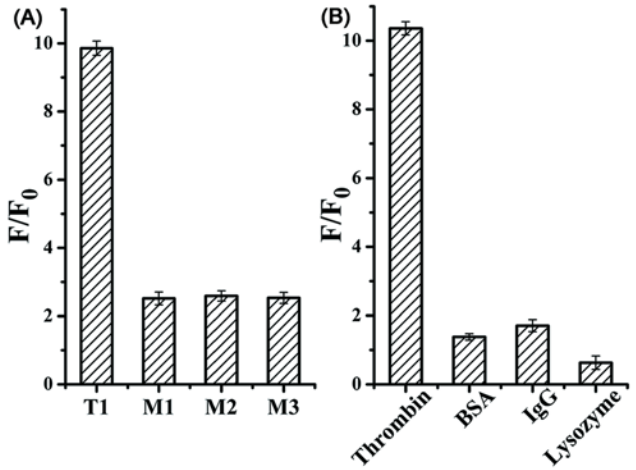

Fig. 8 (A) Fluorescence intensity changes (F/F_0) of P-FAM/NS-1 toward target DNA T1 (25 nM) and three kinds of single-base mismatched DNA M1, M2, M3 (25 nM). (B) Fluorescence intensity changes (F/F_0) of P-FAM/NS-1 toward thrombin (25 nM), BSA (125 nM), IgG (125 nM), and lysozyme (125 nM). F_0 and F are the fluorescence intensity of P-FAM/NS-1 in the absence and presence of the targets.

To test the specificity of the DNA sensor, the single nucleotide polymorphisms (SNPs) analysis was performed (Fig. 8A). In the presence of single-base mismatched DNA, the fluorescence change (F/F_0, F_0 and F are the fluorescence intensity of P-FAM/NS-1 in the absence and presence of the targets.) was little, whereas the presence of T1 demonstrated a significant fluorescence enhancement. As shown in Fig. S10, the addition of triple-base mismatched DNA T2 only led to a slight fluorescence enhancement compared with the blank. These results indicated that the DNA sensor was highly selective. To assess the specificity of the aptamer sensor for thrombin, different proteins (bovine serum albumin (BSA), human IgG, and lysozyme) were chosen as interferents (Fig. 8B). However, none of the three proteins could induce the distinct fluorescence change, even at high concentration (125 nM). This result proved that the sensing platform was highly selective toward thrombin.

Conclusions

In summary, it has been revealed for the first time that bioinspired polydopamine nanospheres possess high fluorescence quenching efficiency and different affinities toward various ssDNA conformations. On the basis of the findings, PDANSs could be employed as a sensing platform for the detection of DNA and proteins. It was demonstrated with good selectivity to specific targets. And this sensing method is fast and simple, without the involvement of other reagents and further operations. In addition, the assay is homogeneous for the assay occurs exclusively in the liquid phase, which makes it easy to automate and suitable for fluorescence imaging. Furthermore, compared to the classic nanoquenchers, PDANSs with tunable diameters can be readily synthesized on a large scale through a facile and low-cost method, and applied without further treatment. With these advantages, this work provides opportunities to develop simple, rapid, and economical biosensors for molecular diagnostics. Because PDA is widely distributed throughout the human body and it can be physically metabolized, PDANSs are highly suited for *in vivo* applications. Moreover, coupled with the reported unique physical and chemical properties, the application of PDA will be broaden.

Experimental

Materials. Dopamine hydrochloride was purchased from Sangon Biotechnology Co., Ltd (Shanghai, China). Immunoglobulin G (IgG) and lysozyme (hen egg white, 70000 u/mg) were purchased from Biosharp, Japan. Bovine serum albumin (BSA) was obtained from Amresco (Solon, USA) and human α-thrombin was ordered from Sigma-Aldrich, USA. All other reagents were of analytical reagent grade and used without further purification. 20 mM Tris-HCl buffer (pH 7.4, containing 140 mM NaCl, 5 mM KCl, 1mM $MgCl_2$ and 1mM $CaCl_2$) was used in this experiment. DNA sequences were synthesized by Sangon, and the sequences were shown in Table 1.

Preparation and characterization of PDANSs. PDANSs were synthesized according to a previous report with some modifications. Briefly, 100 mg dopamine hydrochloride was added to the mixture of 100 mL Tris-buffer (10 mM) and 40 mL isopropyl alcohol with stirring. After stirred for 72 h, NS-1 was obtained. The suspension was centrifuged and washed/resuspended with water for several times. The precipitate was dried for the following experiment. Scanning electron microscope (SEM) images were recorded using an S-4800 scanning electron microscope (Hitachi, Japan). IR spectra were determined by a Nicolet 6700 FT-IR Spectrometer in the range of 400 to 4000 cm^{-1} choosing KBr as medium. Raman spectra were recorded on a Jobin-Yvon HR800 laser Raman spectrometer with 480 nm wavelength incident laser light in the range of 500 to 2000 cm^{-1}. A NanoDrop 2000c Spectrophotometer was used to obtain UV-Visible spectra. Some other PDANSs were also prepared by controlling the molar ratio of buffer to isopropyl alcohol and the reaction time.

Fluorescence quenching measurements. The fluorescence measurements were performed at room temperature on a Shimadzu RF-5301PC fluorophotometer. The excitation and emission wavelength of the fluorophores were shown in Table S1. The emission spectra of probe DNA and the mixture of the probe DNA with PDANSs were recorded. The quenching efficiency (QE) was calculated by the formula: $QE=(1-F_Q/F_I)\times100\%$, where F_Q and F_I are fluorescence intensities in the presence and absence of PDANSs, respectively. The fluorescence quenching kinetic analysis was also conducted. The emission intensity of P-FAM at 518 nm was recorded each 3 s at the excitation of 470 nm after the introduction of PDANSs.

Fluorescence lifetime analysis. The fluorescence lifetime analysis was conducted on an Edinburgh FLS920 Time-Resolved Fluorescence Spectrofluorometer. P-Cy5 and P-Cy5/NS-1 were used for lifetime analysis. The fluorescence decay curves were recorded with the excitation and emission wavelength at 625 and 660 nm, respectively.

Fluorescence anisotropy analysis. The fluorescence anisotropy was examined with the FLS920 fluorescence spectrometer. The fluorescence anisotropies of P-FAM, P-FAM/T1, and P-FAM/Thrombin were measured in the absence and presence of NS-1. Excitation and emission wavelength are 470 and 518 nm, respectively.

Fluorescence assay of DNA and thrombin. Probe DNA P-FAM was mixed with NS-1 for 10 minutes at room temperature as the sensing platform. The target T1 or thrombin was added to this sensing platform, with further incubation at 37 °C for 0.5 - 1.5 hr. The final T1 concentration in the mixture ranged from 0.78 to 200 nM, and the thrombin concentration ranged from 1.56 to 100 nM. After the incubation, the fluorescence of the mixture was detected with the RF-5301PC fluorophotometer. The fluorescence intensity at 518 nm is used for quantitative analysis.

Acknowledgements

We acknowledge financial support of the National Basic Research Program of China (973 Program, 2011CB911003), National Natural Foundation of China (Grant No. 21227009, 21175066 and 21328504), Jiangsu Province Science and Technology Support Program (No. BE2011773), Research Foundation of Jiangsu Province Environmental Monitoring (No. 1116), and the National Science Funds for Creative Research Groups (NO. 21121091).

Notes and references

State Key Laboratory of Analytical Chemistry for Life Science, School of Chemistry and Chemical Engineering, Nanjing University, Nanjing, Jiangsu 210093, China. Fax: +86 25 83595835; Tel: +86 25 83595835; E-mail: xudanke@nju.edu.cn

† Electronic Supplementary Information (ESI) available: detailed procedure of the preparation of PDANSs, optimization of DNA sensor and supplementary figures Fig. S1-S11. See DOI: 10.1039/b000000x/

1. L. Yuan, W. Lin, K. Zheng, L. He and W. Huang, *Chem. Soc. Rev.*, 2013, **42**, 622-661.
2. Y. Yang, Q. Zhao, W. Feng and F. Li, *Chem. Rev.*, 2013, **113**, 192-270.
3. S. Tyagi and F. R. Kramer, *Nat. Biotechnol.*, 1996, **14**, 303-308.
4. D. M. Kolpashchikov, *Chem. Rev.*, 2010, **110**, 4709-4723.
5. N. Dai and E. T. Kool, *Chem. Soc. Rev.*, 2011, **40**, 5756-5770.
6. J. Lei and H. Ju, *Chem. Soc. Rev.*, 2012, **41**, 2122-2134.
7. M. Swierczewska, G. Liu, S. Lee and X. Chen, *Chem. Soc. Rev.*, 2012, **41**, 2641-2655.
8. G. Aragay, F. Pino and A. Merkoci, *Chem. Rev.*, 2012, **112**, 5317-5338.
9. B. Dubertret, M. Calame and A. J. Libchaber, *Nat. Biotechnol.*, 2001, **19**, 365-370.
10. D. J. Maxwell, J. R. Taylor and S. Nie, *J. Am. Chem. Soc.*, 2002, **124**, 9606-9612.
11. H. Li, Y. Zhang, L. Wang, J. Tian and X. Sun, *Chem. Commun.*, 2011, **47**, 961-963.
12. Y. Wang, L. Bao, Z. Liu and D. W. Pang, *Anal. Chem.*, 2011, **83**, 8130-8137.
13. R. Yang, J. Jin, Y. Chen, N. Shao, H. Kang, Z. Xiao, Z. Tang, Y. Wu, Z. Zhu and W. Tan, *J. Am. Chem. Soc.*, 2008, **130**, 8351-8358.
14. N. Nakayama-Ratchford, S. Bangsaruntip, X. Sun, K. Welsher and H. Dai, *J. Am. Chem. Soc.*, 2007, **129**, 2448-2449.
15. C. H. Lu, H. H. Yang, C. L. Zhu, X. Chen and G. N. Chen, *Angew. Chem. Int. Ed.*, 2009, **48**, 4785-4787.
16. R. S. Swathi and K. L. Sebastian, *J. Chem. Phys.*, 2008, **129**, 054703.
17. X. Zhu, H. Zheng, X. Wei, Z. Lin, L. Guo, B. Qiu and G. Chen, *Chem. Commun.*, 2013, **49**, 1276-1278.
18. C. Zhu, Z. Zeng, H. Li, F. Li, C. Fan and H. Zhang, *J. Am. Chem. Soc.*, 2013, **135**, 5998-6001.
19. Y. Tu, W. Li, P. Wu, H. Zhang and C. Cai, *Anal. Chem.*, 2013, **85**, 2536-2542.
20. Y. He, X. Xing, H. Tang and D. Pang, *Small*, 2013, **9**, 2097-2101.
21. Y. Wen, C. Peng, D. Li, L. Zhuo, S. He, L. Wang, Q. Huang, Q. H. Xu and C. Fan, *Chem. Commun.*, 2011, **47**, 6278-6280.
22. C. H. Lu, J. Li, M. H. Lin, Y. W. Wang, H. H. Yang, X. Chen and G. N. Chen, *Angew. Chem.*, 2010, **49**, 8454-8457.
23. H. Jang, Y. K. Kim, H. M. Kwon, W. S. Yeo, D. E. Kim and D. H. Min, *Angew. Chem.*, 2010, **49**, 5703-5707.
24. H. Jang, S. R. Ryoo, Y. K. Kim, S. Yoon, H. Kim, S. W. Han, B. S. Choi, D. E. Kim and D. H. Min, *Angew. Chem. Int. Ed.*, 2013, **52**, 2340-2344.
25. X. Liu, R. Aizen, R. Freeman, O. Yehezkeli and I. Willner, *ACS nano*, 2012, **6**, 3553-3563.
26. L. Cui, X. Lin, N. Lin, Y. Song, Z. Zhu, X. Chen and C. J. Yang, *Chem. Commun.*, 2012, **48**, 194-196.
27. C. Zhang, Y. Yuan, S. Zhang, Y. Wang and Z. Liu, *Angew. Chem. Int. Ed.*, 2011, **50**, 6851-6854.
28. H. Lee, S. M. Dellatore, W. M. Miller and P. B. Messersmith, *Science*, 2007, **318**, 426-430.
29. Y. Liu, K. Ai and L. Lu, *Chem. Rev.*, 2014, DOI: 10.1021/cr400407a.
30. Q. Ye, F. Zhou and W. Liu, *Chem. Soc. Rev.*, 2011, **40**, 4244-4258.
31. D. R. Dreyer, D. J. Miller, B. D. Freeman, D. R. Paul and C. W. Bielawski, *Chemical Science*, 2013, **4**, 3796.
32. J. Cui, Y. Yan, G. K. Such, K. Liang, C. J. Ochs, A. Postma and F. Caruso, *Biomacromolecules*, 2012, **13**, 2225-2228.
33. B. P. Lee, P. B. Messersmith, J. N. Israelachvili and J. H. Waite, *Annu. Rev. Mater. Res.*, 2011, **41**, 99-132.
34. I. You, S. M. Kang, S. Lee, Y. O. Cho, J. B. Kim, S. B. Lee, Y. S. Nam and H. Lee, *Angew. Chem. Int. Ed.*, 2012, **51**, 6126-6130.
35. J. Ryu, S. H. Ku, H. Lee and C. B. Park, *Adv. Funct. Mater.*, 2010, **20**, 2132-2139.
36. S. H. Yang, S. M. Kang, K.-B. Lee, T. D. Chung, H. Lee and I. S. Choi, *J. Am. Chem. Soc.*, 2011, **133**, 2795-2797.
37. H. Lee, B. P. Lee and P. B. Messersmith, *Nature*, 2007, **448**, 338-341.
38. M.-H. Ryou, Y. M. Lee, J.-K. Park and J. W. Choi, *Adv. Mater.*, 2011, **23**, 3066-3070.
39. H. Lee, J. Rho and P. B. Messersmith, *Adv. Mater.*, 2009, **21**, 431-434.
40. J. Yan, L. Yang, M. F. Lin, J. Ma, X. Lu and P. S. Lee, *Small*, 2013, **9**, 596-603.
41. Y. Liu, K. Ai, J. Liu, M. Deng, Y. He and L. Lu, *Adv. Mater.*, 2013, **25**, 1353-1359.
42. S. Hong, Y. S. Na, S. Choi, I. T. Song, W. Y. Kim and H. Lee, *Adv. Funct. Mater.*, 2012, **22**, 4711-4717.
43. D. R. Dreyer, D. J. Miller, B. D. Freeman, D. R. Paul and C. W. Bielawski, *Langmuir*, 2012, **28**, 6428-6435.
44. J. Liebscher, R. Mrowczynski, H. A. Scheidt, C. Filip, N. D. Hadade, R. Turcu, A. Bende and S. Beck, *Langmuir*, 2013, **29**, 10539-10548.
45. M. d'Ischia, A. Napolitano, A. Pezzella, P. Meredith and T. Sarna, *Angew. Chem. Int. Ed.*, 2009, **48**, 3914-3921.
46. K. E. Secor and T. E. Glass, *Org. Lett.*, 2004, **6**, 3727-3730.
47. X. Ji, G. Palui, T. Avellini, H. B. Na, C. Yi, K. L. Knappenberger, Jr. and H. Mattoussi, *J. Am. Chem. Soc.*, 2012, **134**, 6006-6017.
48. I. L. Medintz, M. H. Stewart, S. A. Trammell, K. Susumu, J. B. Delehanty, B. C. Mei, J. S. Melinger, J. B. Blanco-Canosa, P. E. Dawson and H. Mattoussi, *Nat. Mater.*, 2010, **9**, 676-684.
49. Y. Wang, P. Shen, C. Li, Y. Wang and Z. Liu, *Anal. Chem.*, 2012, **84**, 1466-1473.
50. L. Zeng, Y. Yuan, P. Shen, K. Y. Wong and Z. Liu, *Chem. - Eur. J.*, 2013, **19**, 8063-8067.

51. F. Li, H. Pei, L. Wang, J. Lu, J. Gao, B. Jiang, X. Zhao and C. Fan, *Adv. Funct. Mater.*, 2013, **23**, 4140-4148.
52. F. Li, Y. Huang, Q. Yang, Z. Zhong, D. Li, L. Wang, S. Song and C. Fan, *Nanoscale*, 2010, **2**, 1021-1026.
53. S. He, B. Song, D. Li, C. Zhu, W. Qi, Y. Wen, L. Wang, S. Song, H. Fang and C. Fan, *Adv. Funct. Mater.*, 2010, **20**, 453-459.
54. R. Yang, Z. Tang, J. Yan, H. Kang, Y. Kim, Z. Zhu and W. Tan, *Anal. Chem.*, 2008, **80**, 7408-7413.
55. L. Wang, J. Zhu, L. Han, L. Jin, C. Zhu, E. Wang and S. Dong, *ACS nano*, 2012, **6**, 6659-6666.